ASEAN Journal for Science and Engineering in Materials

Journal homepage: https://ejournal.bumipublikasinusantara.id/index.php/ajsem

Upcycling Polymeric Waste into Interpenetrating Polymer Network Adsorbents for Sustainable Wastewater Treatment

*Ghayda Yaseen Al Kindi, Rana J. Kadhim, Elaf Abd Al-Azal Ihsan, Sinan A. Al-Haddad**

University of Technology-Iraq, Iraq
Correspondence: E-mail: sinan.a.alhaddad@uotechnology.edu.iq

ABSTRACT

This study reports the sustainable synthesis, characterization, and application of Interpenetrating Polymer Networks (IPNs) derived from post-consumer polystyrene kitchenware and epoxy resin residues as a cost-effective adsorbent for amoxicillin removal from wastewater. The conversion of these polymeric wastes into functional materials aligns with circular economy strategies. Batch adsorption experiments were carried out to examine the effects of key operational parameters, including adsorbent dosage, contact time, and solution pH. The results showed a maximum removal efficiency (96%) at an adsorbent dosage of 0.1 g and pH 5. Kinetic analysis indicated that the adsorption process followed a pseudo-second-order model, suggesting chemisorption as the dominant mechanism, with an equilibrium adsorption capacity (qe) of 8.13 mg/g. Isotherm modeling demonstrated that the Langmuir model provided the best fit, confirming monolayer adsorption on a homogeneous surface, while Temkin parameters indicated favorable adsorption energetics. Overall, these findings highlight the potential of waste-derived IPNs as eco-friendly and highly effective materials for removing pharmaceutical contaminants from aqueous environments, contributing to the advancement of sustainable wastewater treatment technologies.

ARTICLE INFO

Article History:
Submitted/Received 05 Apr 2025
First Revised 01 May 2025
Accepted 01 Jul 2025
First Available online 01 Oct 2025
Publication Date 01 Mar 2026

Keyword:
Adsorption,
Batch reactor,
Epoxy resin,
Pharmaceutical waste,
Polystyrene.

1. INTRODUCTION

Pharmaceutical contamination in aquatic and terrestrial environments has become a pressing issue in environmental science and chemical engineering (Ibrahim *et al*., 2023; Lin *et al*., 2024; Singh *et al*., 2022). With the continued growth of industrial output, medical consumption, and agricultural intensification, increasing amounts of micropollutants—including pharmaceuticals—are being released into ecosystems (Hu *et al*., 2025; Jin *et al*., 2025; Lee *et al*., 2025; Mondal *et al*., 2025; Wang *et al*., 2025). Classified as "contaminants of emerging concern" (CECs), these substances persist in water bodies, sediments, and soils, threatening ecological balance and human health (Adeel *et al*., 2025; Codina *et al*., 2025; Yang *et al*., 2025). Their resistance to conventional degradation pathways, bioaccumulative properties, and pharmacologically active structures underscore the need for advanced treatment strategies (Hayouni *et al*., 2025; Munyengabe *et al*., 2025). In response, recent research has increasingly emphasized low-cost, sustainable, and waste-derived approaches for mitigating pollutants in wastewater, highlighting adsorption-based technologies and the development of innovative functional materials (Kargule *et al*., 2025; Mohammed *et al*., 2025; Sheng *et al*., 2023).

Over the past three decades, pharmaceutical residues have been detected in nearly every environmental matrix worldwide, including surface water, groundwater, soils, and sediments (Alenzi *et al*., 2021; Gao *et al*., 2024). These residues arise from multiple sources, such as domestic consumption, hospital effluents, veterinary applications, and pharmaceutical manufacturing waste. Designed to exert biological activity, pharmaceuticals—whether naturally derived or synthetically produced—contain active constituents such as diclofenac, tetracycline, and amoxicillin, which are widely used in both human and veterinary medicine, with or without prescription.

Elevated concentrations of pharmaceutical compounds (particularly those containing organic constituents) have been frequently detected in surface waters, raising serious concerns for both human health and aquatic ecosystems. Numerous studies have documented their occurrence across diverse environmental media, including receiving waters, sewage sludge, municipal and industrial wastewater, coastal zones, and even surface and groundwater systems (Laksaci *et al*., 2023). Effluents from wastewater treatment plants are recognized as a major pathway for the discharge of hazardous pharmaceutical residues into natural water bodies. The persistence of these compounds, often linked to their high hydrophilicity and low biodegradability, greatly limits their removal by conventional treatment processes. Insufficient removal can lead to the structural transformation or degradation of parent compounds, which may compromise cellular and physiological functions in humans through exposure via food, water, or air pathways (Fraiha *et al*., 2024).

Various treatment technologies have been investigated to mitigate pharmaceutical contamination, with the choice of method largely depending on the nature of the pollutant and specific treatment objectives. For example, the effective adsorption of diclofenac from synthetic wastewater using commercial activated carbon (Chai *et al*., 2021). Similarly, the potential of Moringa Oleifera seed powder as a natural adsorbent for ibuprofen removal in a batch reactor system (Al-Kindi & Al-Haidri, 2021). Another study utilized Al-Fe pillared clay under three configurations (coagulation, adsorption, and a hybrid approach), finding that the hybrid method achieved the highest removal efficiency for tetracycline (Al-Kindi and Alnasrawy, 2022). More recently, an advanced electrochemical technique employing two- and three-dimensional systems, enhanced with nano-zero valent iron (nZVI) derived from

orange peel extract and stabilized with carboxymethyl cellulose (CMC) as granular electrodes, to successfully eliminate tetracycline (Al-Kindi and Al-Haidri, 2023).

An interpenetrating polymer network (IPN) represents a promising recent approach for pollutant removal. This material consists of two or more polymer networks that are physically interlaced but not covalently bonded, enabling the coexistence of multiple reactive functional groups in proximity. Such groups can donate electrons and form stable coordination interactions with contaminant ions, thereby enhancing adsorption performance (Radu *et al*., 2014). Interestingly, IPNs can be synthesized from waste polymers commonly found in household kitchen items, including disposable cups, food containers, and drinking glasses. These products are typically made of polystyrene (PS), polyethylene (PE), and polypropylene (PP)—thermoplastic polymers derived from aromatic hydrocarbons. According to ASTM standards, these polymers are classified as non-biodegradable, meaning they persist in the environment and accumulate in terrestrial and aquatic ecosystems, particularly along beaches and waterways. The environmental concerns are further heightened when these polymers come into contact with hot food or liquids, as they can release free radicals and chemical residues associated with severe health risks, including carcinogenic effects. Moreover, many of these plastics may contain bisphenol A (BPA), an endocrine disruptor known to cause significant harm to human health.

Epoxy resins are extensively used in construction and industrial applications, including grouting, adhesives, coatings, and composite materials. Their popularity stems from desirable properties such as high compressive and tensile strength, strong adhesion, long-term durability, chemical resistance to acids, alkalis, and organic solvents, and minimal shrinkage during curing. Despite these advantages, epoxy resins (like many aromatic polymers) pose environmental concerns due to their low biodegradability and resistance to conventional degradation processes. When combined with other non-biodegradable polymers, such as polystyrene from disposable food containers, their accumulation significantly contributes to persistent plastic pollution. To address this issue, the present study introduces a novel approach: synthesizing interpenetrating polymer networks (IPNs) by integrating polystyrene waste with epoxy resin. This strategy aims to transform waste polymers into a low-cost, eco-friendly adsorbent material for the removal of pharmaceutical contaminants. Specifically, the study focuses on eliminating amoxicillin from the wastewater of the Al-Jazeera Pharmaceutical Factory (amoxicillin production line) using a batch reactor system.

Despite extensive efforts to remove pharmaceutical contaminants from wastewater through physical, chemical, and biological methods, many existing approaches face significant challenges, including high operational costs, intensive energy requirements, limited reusability of adsorbents, and low efficiency in treating complex pollutant mixtures. In addition, numerous synthetic adsorbents are produced from non-renewable sources and exhibit poor biodegradability, leading to secondary pollution risks. These drawbacks highlight the urgent need for adsorbent materials that are cost-effective, sustainable, and highly efficient, while also contributing to both environmental protection and solid waste management. In response, the present study proposes a novel IPN-based adsorbent synthesized from waste-derived materials. The main contributions of this work are as follows:

(i) Development of a novel waste-to-resource strategy by converting disposable polystyrene food containers and epoxy resin waste into a functional IPN-based adsorbent, thereby addressing plastic pollution while reducing material costs.

(ii) First demonstration of PS–epoxy IPNs for pharmaceutical wastewater treatment, specifically for the removal of amoxicillin from real industrial effluents, to the best of current knowledge.
(iii) Validation of adsorption performance and mechanism, with the synthesized IPNs exhibiting high adsorption efficiency under optimized conditions, supported by kinetic and isotherm modeling that confirmed a chemisorption mechanism and monolayer adsorption behavior.

2. METHOD

2.1. Materials

The primary materials employed for the glycolysis of polystyrene were zinc acetate ($Zn(CH_3COO)_2$), a white crystalline salt used as a catalyst, and ethylene glycol, which acted both as a depolymerizing agent and a viscosity modifier. Disposable polystyrene plates were collected and utilized as the solid polymer waste source. All chemicals were of analytical grade and were obtained from local suppliers without any further purification.

2.2. The Preparation of an Interconnected Polymer Network (IPNS)

The interpenetrating polymer network (IPN) was synthesized via a two-step process: (i) glycolysis of waste polystyrene and (ii) subsequent integration of the glycolyzed product with epoxy resin to form the final crosslinked network. This approach was specifically designed to upcycle non-biodegradable polystyrene waste while chemically incorporating it into an epoxy-based matrix, thereby producing a stable and functional adsorbent material suitable for the removal of pharmaceutical contaminants.

2.2.1. Stage 1: Using glucose in the analysis of polystyrene

Disposable polystyrene kitchen plates were first washed with distilled water, dried, and cut into 1 × 1 cm pieces. The glycolysis process was carried out in a 500 mL double-necked flask, as illustrated in **Figure 1**. A thermometer was inserted into one neck, while a condenser was fitted into the other. A total of 5 g of cut polystyrene was introduced into the flask along with 0.18 g of zinc acetate, which served to prevent the material from adhering to the vessel walls (Harris *et al*., 2022). Subsequently, 20 mL of ethylene glycol was added to enhance viscosity, promote free radical formation, reduce polymer solubility, and slow down the degradation reaction. The reaction mixture was then heated to 180 °C and maintained for 6 hours under continuous stirring with a magnetic stirrer. Upon completion, 50 mL of distilled water was added, and the mixture was rapidly cooled in an ice bath for 2 hours. The resulting precipitate was collected, dried, and ground into fine powder using a plastic grinder.

2.2.2. Stage 2: Preparation of an IPN

The interpenetrating polymer network (IPN) was prepared by combining 5 g of the ground glycolyzed polystyrene precipitate (obtained from the previous step) with 5 g of epoxy resin, followed by the addition of an amine curing agent. The mixture was then placed in a drying oven at 100 °C for 1 hour to promote polymer hardening and enhance network cohesion. Subsequently, the temperature was reduced to 70 °C and maintained for an additional 30 minutes to complete the curing process, resulting in the formation of the IPN structure. The overall preparation procedure is illustrated in **Figure 1**.

To characterize the physicochemical properties and evaluate the adsorption potential of the synthesized IPNs, several analytical techniques were employed. Fourier-transform infrared spectroscopy (FTIR) was used to identify the functional groups within the polymer

network. The surface morphology and pore structure were examined using scanning electron microscopy (SEM). In addition, zeta potential measurements were carried out to determine the surface charge of the IPNs in aqueous suspension, a parameter that critically influences electrostatic interactions during the adsorption of pharmaceutical compounds.

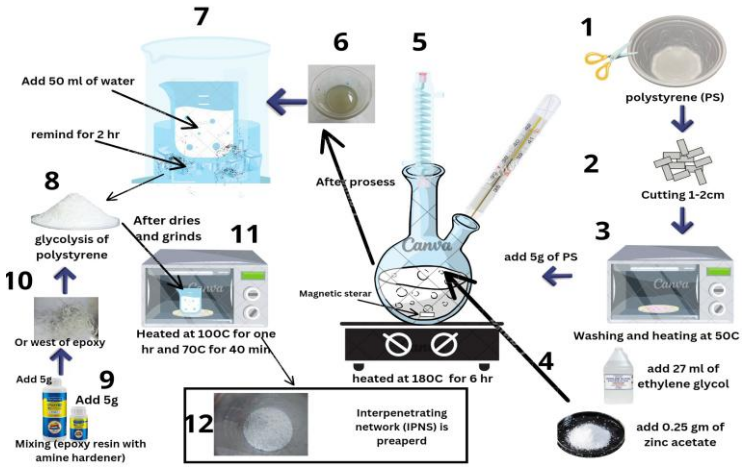

Figure 1. Process for the preparation of IPNS.

2.3. Determination of Amoxicillin Absorbance

The UV-visible spectrophotometric method was employed to determine the absorbance of amoxicillin within the spectral range of 200–800 nm, as illustrated in **Figure 2**. Based on Beer's law, calibration was performed using standard amoxicillin solutions with concentrations ranging from 1 to 50 mg/L. The calibration curve relating concentration to absorbance indicated that the maximum absorbance occurred at 280 nm, which was selected as the analytical wavelength for subsequent measurements (**Figure 3**).

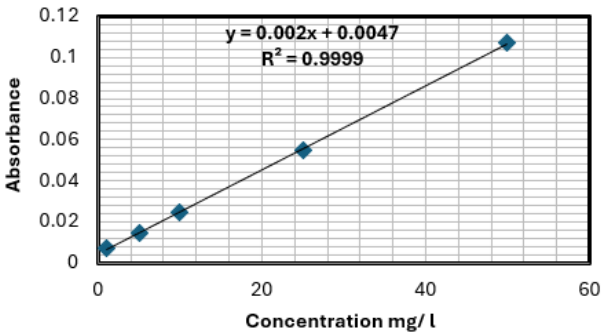

Figure 2. UV spectrophotometer calibration of amoxicillin solution (0.01 M).

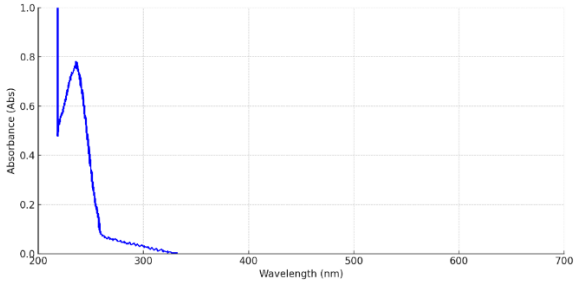

Figure 3. The 200–800 nm spectral region of the carving for amoxicillin.

2.4. Adsorption Analysis

A wastewater sample was collected from the amoxicillin production line of Al Jazeera Laboratory, and the initial amoxicillin concentration was determined to be 25 mg/L using a UV–visible spectrophotometer. To evaluate the efficiency of IPNs in amoxicillin removal and to optimize operational conditions, batch reactor experiments were conducted under varying parameters, including initial amoxicillin concentration, IPN dosage, solution pH, and contact time. In contrast, other parameters, such as mixing velocity and temperature, were kept constant. Kinetic studies were also performed to gain insights into the adsorption mechanism and rate-controlling steps (Fraiha *et al*., 2024). The adsorption kinetics were analyzed using the pseudo-first-order and pseudo-second-order models, as described in Equations (1) and (2) (Kindi *et al*., 2025; Laksaci *et al*., 2023).

$$(First\ -order)\ log\ (qe\ -\ qt)\ =\ log\ qe\ -\ K1t \quad (1)$$

$$(Second\ -\ order)\ \frac{t}{qt} = \frac{1}{K_2\ qe^2} + \frac{t}{qe} \quad (2)$$

Where, t is the time of the adsorption process (min), q^t and q_e are the amounts adsorbed at time t and equilibrium (mg/g), where the rate constants for pseudo-first- and pseudo-second-order reactions are k1 and k2, determined from plotting ln ($q_e - q_t$) vs t, yields the constant K1 in min^{-1}.

$$Ln\ qe\ =\ ln\ K\ + \frac{1}{n} \times\ lnCe \quad (3)$$

In the Freundlich model, the constant k represents the adsorption capacity, while 1/n (ranging between 0 and 1) indicates adsorption intensity and surface heterogeneity. For the Langmuir model, the slope of the linearized equation was used to determine the adsorption constant, with Equation (4) applied for data fitting and linearization.

$$\frac{1}{qe} = \frac{1}{q_{max}} + \frac{1}{q_{max}.b} * \frac{1}{Ce} \quad (4)$$

The Temkin model has been utilized in the following formula in Equation (5).

$$qe\ =\ \beta\ ln\ \alpha\ +\ \beta\ ln\ Ce \quad (5)$$

where β = (RT/b), R (8.314 J/mol K) is the universal gas constant, T is the absolute temperature in Kelvin, and b is the Temkin constant (J/mg); α and β are calculated from the linear plot of qe vs. ln Ce, which represent slope and intercept.

3. RESULTS AND DISCUSSION

3.1. IPNS Characteristics Results

3.1.1. Fourier-Transform Infrared Spectroscopy (FTIR) Analysis

The FTIR spectrum of the synthesized IPNs, shown in **Figure 4**, exhibits several distinct absorption bands corresponding to functional groups incorporated during polymer network formation. A broad and intense peak at 3444.87 cm^{-1} is assigned to the O–H stretching vibration, indicating the presence of hydroxyl groups introduced during the glycolysis of polystyrene with ethylene glycol. The characteristic C–H stretching vibration of methylene (–CH_2) groups appears at 2877.79 cm^{-1}, confirming the aliphatic backbone of the polymer matrix. Two sharp peaks at 1714.72 and 1685.79 cm^{-1} correspond to C=O stretching vibrations, suggesting the presence of ester or carbonyl functionalities, possibly resulting from oxidation or residual epoxy structures. Additional carbonyl-related absorptions are observed at 1651.07, 1606.70, and 1584.48 cm^{-1}, which may reflect different degrees of conjugation or hydrogen bonding. Furthermore, aromatic C=C stretching vibrations at 1508.33 and 1456.25 cm^{-1} are characteristic of the aromatic rings in the polystyrene component of the network.

A prominent absorption band at 1249.87 cm^{-1} is attributed to C–N stretching, indicating successful crosslinking between polystyrene fragments and the epoxy resin via nitrogen-containing linkers. Symmetric and asymmetric C–O–C ether vibrations are observed at 1132.21 cm^{-1} and 1012.63 cm^{-1}, confirming the incorporation of epoxy-derived structures into the network. Additional fingerprint bands at 873.75, 827.45, 725.23, and 603.72 cm^{-1} further substantiate the complex aromatic and aliphatic character of the synthesized IPNs. Collectively, these functional groups confirm the successful formation of a chemically rich interpenetrating polymer network, which is anticipated to enhance the material's adsorption performance toward pharmaceutical contaminants, such as amoxicillin.

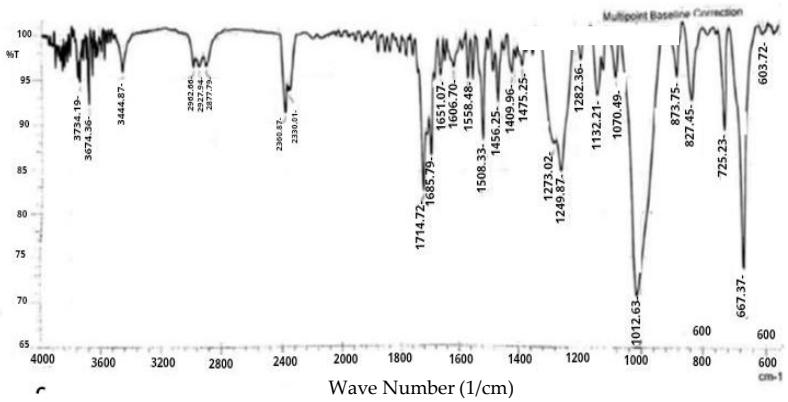

Figure 4. FTIR spectrum of IPNs synthesized from polystyrene and epoxy resin.

3.1.2. Analysis of Zeta Potential

Zeta potential analysis was conducted to evaluate the surface charge of IPN particles in solution, serving as an important indicator of the stability of dispersed particles. The measured zeta potential was −30 mV, as shown in **Figure 5**, indicating the onset of a relatively stable state. Values below −30 mV suggest increased electrostatic repulsion between particles, which enhances dispersion stability. This surface charge facilitates electrostatic attraction between amoxicillin molecules and the IPN surface, thereby improving adsorption capacity. Conversely, when the zeta potential ranges from −30 to +60 mV, the electrostatic interaction between amoxicillin and the IPNs diminishes, resulting in a relatively constant adsorption capacity. When the zeta potential exceeds +60 mV, electrostatic repulsion predominates, leading to a significant reduction in adsorption efficiency (Chen *et al*., 2015).

Changes in zeta potential in the presence of polymers can arise from three primary effects: (i) the transfer of charge from functional groups to the surface of the solid, (ii) the movement or sliding of large adsorbed particles along the surface, and (iii) the displacement of counterions in the Stern layer as a result of polymer adsorption.

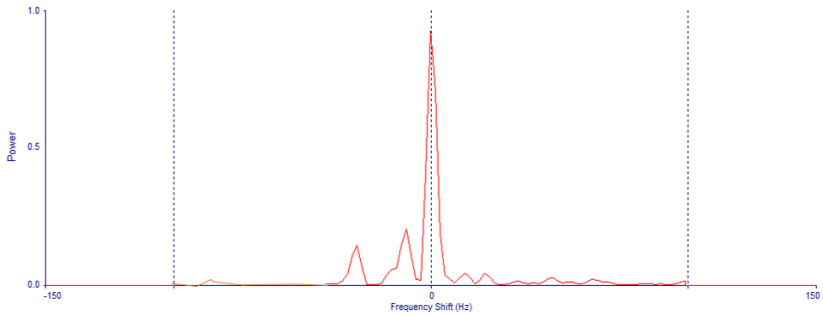

Figure 5. Zeta potential analysis.

3.1.3. SEM

Figure 6 shows the SEM image of the synthesized IPN hydrogel at a magnification of 24,000×, captured using an accelerating voltage of 30.00 kV and a working distance of 25.9 mm. The surface morphology reveals a rough, porous, and heterogeneous microstructure, indicating successful physical integration between polystyrene and epoxy resin during IPN formation. The presence of micron-scale particle clusters suggests significant agglomeration and demonstrates structural compatibility between the two polymer phases.

The hydrogel surface is characterized by interconnected, irregularly shaped cavities with estimated pore sizes ranging from 30 to 80 µm, supporting the material's ability to adsorb pharmaceutical compounds such as amoxicillin. These open and wrinkled pore structures likely arise from electrostatic interactions and hydrogen bonding during crosslinking, which enhance the internal surface area and facilitate diffusion and entrapment of drug molecules. The observed texture and pore distribution are consistent with previous reports, confirming the suitability of IPNs as an effective adsorbent medium for wastewater treatment (Dragan, 2014).

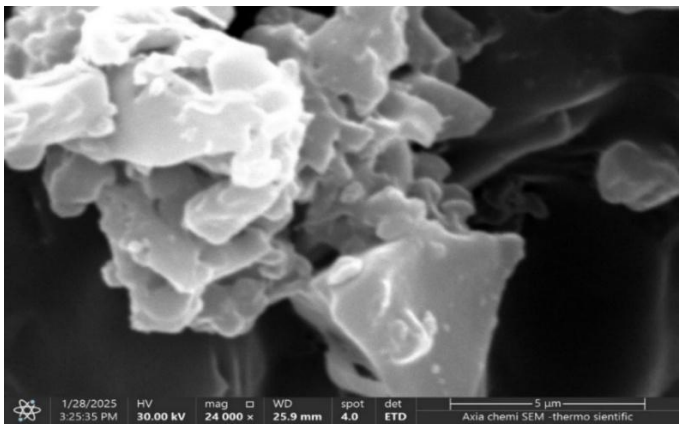

Figure 6. SEM Image of synthesized IPNs hydrogel at 24,000× magnification (Scale: 5 µm).

3.2. Results of Batch Reactor

3.2.1. Effect of contact time

Figure 7 illustrates the temporal dynamics of amoxicillin adsorption onto IPNs, showing both the concentration decrease (mg/L) and removal efficiency (%). The adsorption experiment was conducted using an initial amoxicillin concentration of 25.1 mg/L with 0.1 g of IPNs at neutral pH (7.3), stirred at 200 rpm under room temperature conditions.

As shown in Figure 7a, the amoxicillin concentration dropped sharply from 25.1 mg/L to 10.3 mg/L within the first 10 minutes, indicating a rapid adsorption phase. By 30 minutes, the concentration further decreased to 7.9 mg/L, and after 60 minutes, it reached 6.2 mg/L. The concentration continued to decline gradually, stabilizing around 4.1 mg/L at 360 minutes, suggesting that adsorption equilibrium was achieved. Correspondingly, Figure 7b shows the removal efficiency increasing rapidly from 0% to 58.9% within the first 10 minutes. By 30 minutes, efficiency rose to 68.5%, reaching 75.2% after 60 minutes. The rate of increase slowed thereafter, with removal efficiencies of 78.6% at 180 minutes and 82.3% at 360 minutes, indicating that the majority of adsorption occurred within the first hour.

These results highlight the high affinity of the synthesized IPNs for amoxicillin, particularly during the initial rapid uptake phase. The fast adsorption kinetics can be attributed to the abundance of active sites and the accessible porous structure of the IPNs, whereas the

subsequent plateau indicates either the saturation of available adsorption sites or a slower intraparticle diffusion process at later stages.

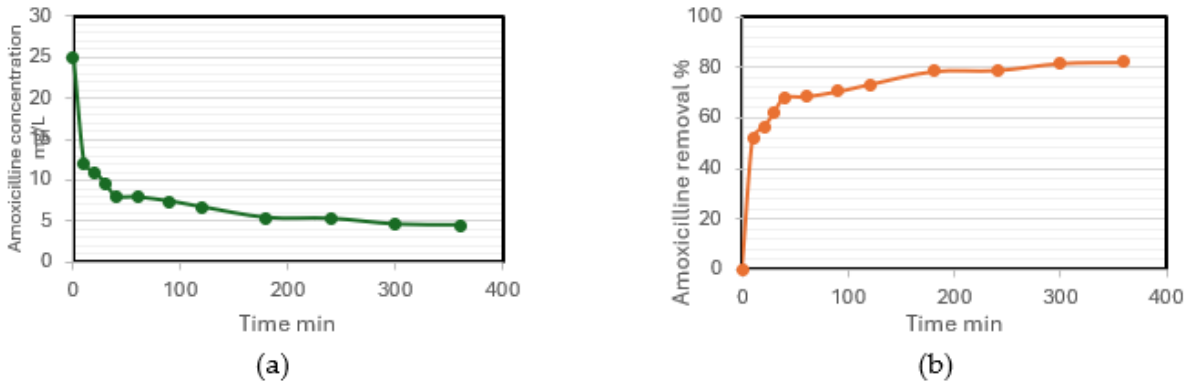

Figure 7. Effect of: (a) contact time on amoxicillin adsorption on IPNS; (b) removal efficiency of amoxicillin adsorption on IPNS.

3.2.2. Effect of pH change on amoxicillin removal on IPNS

The pH of the solution plays a critical role in the efficiency of amoxicillin removal using IPNs, as it influences both the surface charge of the adsorbent and the ionization state of the drug molecules. In this study, batch experiments were conducted using a jar test apparatus (**Figure 8**), with the pH varied from 2 to 9. The initial amoxicillin concentration was 25 mg/L, with an IPN dosage of 0.1 g, agitation at 200 rpm, and room temperature conditions. The corresponding results are presented in **Figure 9**.

Figure 9(a) shows the temporal profile of amoxicillin concentration (mg/L) at different pH levels. In all cases, the initial concentration decreased rapidly within the first 20 minutes. At pH 2, the concentration dropped from 25 mg/L to approximately 9.2 mg/L at 20 minutes and stabilized around 6.0 mg/L after 240 minutes. At pH 5, the removal was most effective, with the concentration reaching 3.2 mg/L at the end of the experiment. For pH 7 and pH 9, the concentration plateaued at 4.4 mg/L and 5.1 mg/L, respectively, indicating moderately high removal efficiencies. **Figure 9(b)** illustrates the corresponding removal efficiencies over time. At pH 2, the efficiency reached approximately 72% at 240 minutes. In contrast, pH 5 exhibited the highest removal efficiency, achieving 88% at equilibrium. At pH 7 and 9, the efficiencies were about 82% and 79%, respectively. These results indicate that a slightly acidic environment (pH 5) provides optimal conditions for interaction between amoxicillin molecules and the active sites of the IPNs. This can be attributed to the minimization of electrostatic repulsion between positively charged amoxicillin and the adsorbent surface, allowing stronger adsorption. At lower pH (e.g., 2), excess hydronium ions likely compete with drug molecules for active sites, reducing adsorption efficiency. These findings are consistent with previous reports, confirming that pH 5 represents the most favorable operational condition for amoxicillin removal using the synthesized IPNs (Al-Kindi *et al*., 2021; Laksaci *et al*., 2023).

Figure 8. Schematic representation of the jar test setup used for batch adsorption experiments.

3.2.3. Effect of amoxicillin concentration change on amoxicillin removal on IPNS

Figure 10 illustrates the effect of varying initial amoxicillin concentrations on its adsorption using the synthesized IPNs, under conditions of pH 5, 0.1 g IPN dosage, and 200 rpm agitation at room temperature. As shown in **Figure 10(a)**, the adsorption process exhibited a rapid decline in concentration within the first 30 minutes across all tested levels. For the 5 mg/L sample, the concentration decreased from 5.1 mg/L to 0.9 mg/L within the first 60 minutes and stabilized around 0.45 mg/L after 240 minutes. At 25 mg/L, the concentration dropped sharply from 25.2 mg/L to 6.7 mg/L in the first 60 minutes, followed by a slower decline to 4.6 mg/L by 360 minutes. For the 35 mg/L case, the concentration fell from 36.4 mg/L to 9.4 mg/L in the first hour, eventually stabilizing near 7.1 mg/L.

Figure 10(b) shows that the removal efficiency (%) inversely correlates with the initial amoxicillin concentration. The 5 mg/L sample achieved the highest efficiency of 91.2% after 360 minutes, followed by 88.0% for 25 mg/L, and 82.85% for 35 mg/L. Most adsorption occurred within the first 50 minutes, during which removal efficiencies rose from 0% to approximately 73, 66, and 58% for the 5, 25, and 35 mg/L samples, respectively. These differences are attributed to the saturation of available adsorption sites: at lower concentrations, a greater proportion of active sites is available per molecule, enhancing adsorption efficiency, whereas higher concentrations lead to competitive interactions that reduce the adsorption rate and overall efficiency. These observations are consistent with previous studies (Al-Kindi & Al-Haidri, 2021; Al-Kindi & Alnasrawy, 2022), confirming that lower initial concentrations favor maximum removal performance when using IPNs.

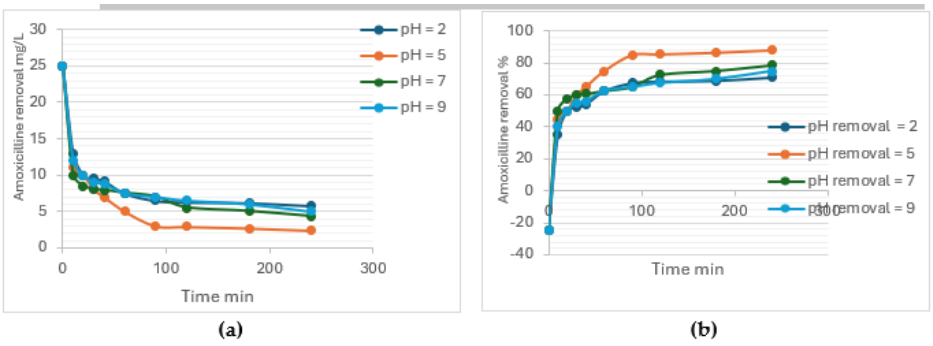

Figure 9. Effect of pH on amoxicillin: (a) concentration (mg/L) versus contact time using IPNs; (b) removal efficiency (%) versus contact time using IPNs.

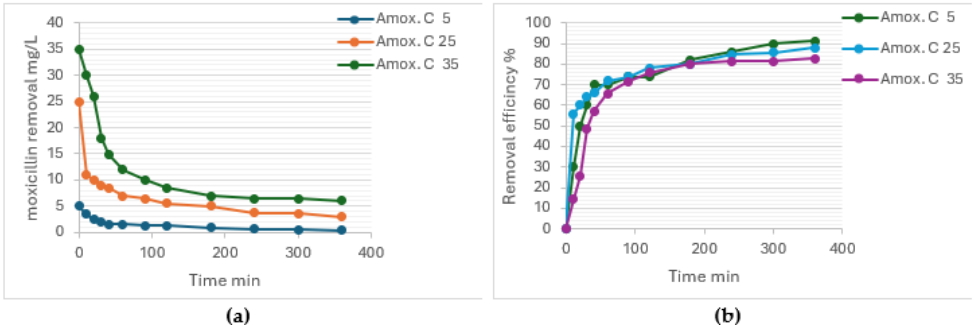

Figure 10. Influence of initial amoxicillin concentration on adsorption behavior and efficiency using IPNS: (a) variation of amoxicillin concentration (mg/l) with time at different initial concentrations; (b) corresponding removal efficiency (%) over time for 5, 25, and 35 mg/l initial concentrations.

3.2.4. Effect of IPNS dosage change on amoxicillin removal

To evaluate the effect of adsorbent dosage on amoxicillin removal, three different IPN dosages (0.01, 0.05, and 0.1 g) were tested at a fixed initial amoxicillin concentration of 5 mg/L, pH 5, and 200 rpm stirring at room temperature. The results, presented in **Figure 11**, demonstrate the significant influence of adsorbent quantity on removal efficiency. As shown in **Figure 11(a)**, higher IPN doses led to a more rapid decrease in amoxicillin concentration. At 30 minutes, the residual concentrations were 2.85, 1.48, and 0.68 mg/L for the 0.01, 0.05, and 0.1 g doses, respectively. By 90 minutes, when near-equilibrium was reached, the concentrations further decreased to 1.81, 0.91, and 0.21 mg/L, respectively, highlighting the critical role of adsorbent dose in enhancing adsorption performance.

Figure 11(b) illustrates the corresponding removal efficiencies over time. At 10 minutes, the removal efficiencies were 44, 61, and 76% for IPN dosages of 0.01, 0.05, and 0.1 g, respectively. These efficiencies continued to increase and plateaued around 150 minutes, reaching 82.5, 87.9, and 96.8%, respectively. The highest efficiency of 96.8% observed with the 0.1 g dose is attributed to the saturation of active sites, which maximized interactions between amoxicillin molecules and the adsorbent. The superior performance at higher dosages is primarily due to the increased availability of surface area and active binding sites, enhancing contact between amoxicillin and the IPNs and improving adsorption kinetics. This effect is particularly pronounced during the initial 30-60 minutes, where the removal curves exhibit the steepest gradients. Additionally, higher dosages reduce the time required to reach equilibrium, as the greater availability of active sites accelerates the adsorption process.

These findings align with established adsorption principles, where the solid-liquid interface becomes quickly saturated at low adsorbent doses but remains underutilized at higher dosages, allowing deeper penetration of amoxicillin molecules into the hydrogel matrix. Increasing the adsorbent dosage also enhances the diffusion process, facilitating nearly complete removal of the solute from the aqueous phase.

3.3. Kinetic and Isotherm Models

3.3.1. Kinetic model results

The adsorption kinetics of amoxicillin onto IPNs were analyzed using both pseudo-first-order and pseudo-second-order models to elucidate the underlying adsorption mechanism. The results, shown in **Figure 12**, reveal notable differences in model fitting and adsorption behavior. For the pseudo-first-order model (**Figure 12(a)**), linear regression yielded a rate

constant of k_1 = 0.0005 min^{-1}, an equilibrium adsorption capacity q_e = 1.1951 mg/g, and a coefficient of determination R^2 = 0.8105. The relatively low R^2 value indicates a poor fit between the model and experimental data. Furthermore, the underestimation of the equilibrium adsorption capacity suggests that the pseudo-first-order model does not adequately describe the adsorption of amoxicillin on IPNs, likely because it assumes physisorption and does not account for chemisorption interactions that may dominate the process.

In contrast, the pseudo-second-order model (**Figure 12b**) demonstrated a substantially better fit with the experimental data. The calculated equilibrium adsorption capacity was q_e = 8.1342 mg/g, nearly seven times higher than that predicted by the pseudo-first-order model, and closely matching experimental observations from earlier figures (e.g., removal capacities at initial concentrations of 5–25 mg/L). The rate constant for the pseudo-second-order model was k_2 = 0.314 min^{-1}, approximately 628 times greater than that obtained for the first-order model. Additionally, the model exhibited an excellent coefficient of determination (R^2 = 0.9624), confirming strong linearity and superior predictive capability compared to the first-order model. The high R^2 value, together with the substantially greater q_e and k_2, indicates that the adsorption process follows pseudo-second-order kinetics and is primarily governed by chemisorption. This involves the formation of chemical bonds (likely hydrogen bonding or electron sharing) between the active functional groups on the IPNs matrix and the amoxicillin molecules. Consequently, the rate-limiting step is not purely diffusion-controlled but involves chemical interactions, which aligns with the rapid initial adsorption observed in prior time-based experiments (**Figures 9** and **13(a)**), where over 70% removal occurred within the first 60 minutes. In summary, both the numerical analysis and model fitting confirm that the pseudo-second-order kinetic model provides a more accurate and mechanistically relevant description of amoxicillin adsorption onto IPNs, highlighting the dominant role of chemisorption.

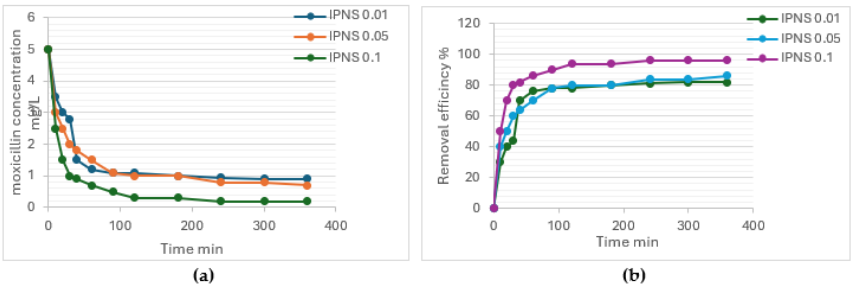

Figure 11. Effect of IPNS dosage on amoxicillin adsorption: (a) concentration decline over time; (b) removal efficiency progression.

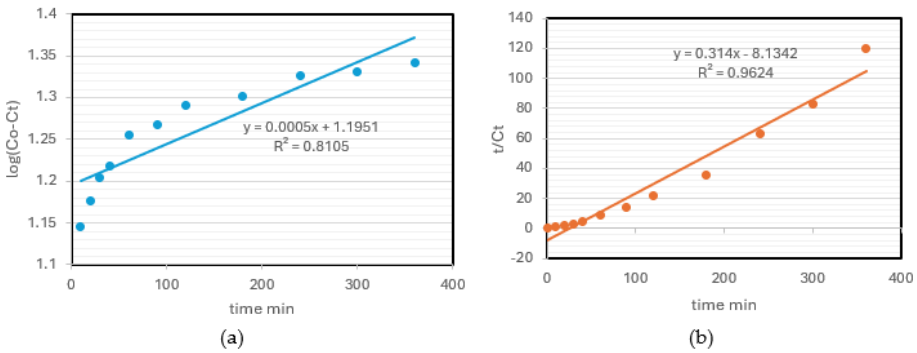

Figure 12. Kinetics for adsorption of amoxicillin onto IPNS for: (a) Pseudo 1st order; (b) Pseudo 2nd order.

3.3.2. Isotherm model constant

Figure 13 presents the isotherm model fits for amoxicillin adsorption onto IPNs, including the Freundlich (**Figure 13(a)**), Langmuir (**Figure 13(b)**), and Temkin (**Figure 13(c)**) models. In the Freundlich plot (**Figure 13(a)**), a strong linear correlation was observed between log q_e and log C, with a slope of approximately −0.8019 and an intercept near −14.453. The coefficient of determination, R^2 = 0.9373, indicates a very good fit. These results suggest that adsorption occurs on a heterogeneous surface, consistent with multilayer adsorption behavior. The data points, ranging from log C ≈ −18.6 to −19.6 and log q_e ≈ 0.6 to 1.1, display a consistent distribution along the linear trendline, reinforcing the suitability of the Freundlich model for describing the adsorption characteristics of the system.

In contrast, the Langmuir model (**Figure 13(b)**) showed a comparatively poor fit, with an R^2 value of only 0.6793. The data points of C_e (ranging approximately from 0 to 30 mg/L) versus C_e/q_e (from −0.6 to −0.1) display a scattered distribution around the linear trendline. The slope and intercept values of −0.0192 and −0.1817, respectively, indicate that the Langmuir model inadequately represents monolayer adsorption, suggesting that the active sites on the IPNs surface are not uniform and limiting the applicability of Langmuir assumptions in this system. The Temkin model (**Figure 13(c)**), however, demonstrated the best statistical performance, with an R^2 of 0.947. The plot of q_e versus log C_e shows a relatively narrow x-axis range (1.1–1.35) and a corresponding q_e range of 0.4–1.2 mg/g. The data follow a tightly clustered linear trend, with a slope of −2.8088 and an intercept of 4.3233, indicating a strong correlation between adsorption capacity and the logarithm of equilibrium concentration. This suggests that interactions between the adsorbent and adsorbate decrease linearly with coverage, consistent with the assumptions of the Temkin model. In summary, isotherm evaluation indicates that the Temkin model provides the most accurate predictive fit for amoxicillin adsorption onto IPNs, followed closely by the Freundlich model, whereas the Langmuir model is the least representative based on both linearity and data distribution. These findings are in agreement with previous reports (Liu *et al*., 2012).

The adsorption performance of amoxicillin onto IPNs was further evaluated using three equilibrium isotherm models (Langmuir, Freundlich, and Temkin) as summarized in **Table 1**. Among these, the Langmuir model exhibited the highest correlation coefficient (R^2 = 0.947), indicating an excellent fit to the experimental data. This suggests that the adsorption process predominantly follows monolayer adsorption on a relatively homogeneous surface. The Langmuir constant, K_l = 0.8019 L/mg, indicates a strong affinity between amoxicillin molecules and the active sites on the IPNs surface. However, the calculated RL value of 14.453 (typically used to assess adsorption favorability) requires cautious interpretation. Values of RL > 1 usually suggest unfavorable adsorption, which seems inconsistent with the high R^2 and the experimentally observed high removal efficiencies. This discrepancy may arise from limitations in the RL parameter under the specific experimental conditions or scale, highlighting that RL should be considered alongside other model parameters and empirical observations when evaluating adsorption behavior.

In comparison, the Freundlich model, which describes multilayer adsorption on heterogeneous surfaces, exhibited a much lower correlation coefficient (R^2 = 0.6793), indicating a poor fit relative to the other models. The Freundlich constants further reflect weaker adsorption characteristics: Kf = 0.0192 mg/g·(L/mg)1/n suggests a very low adsorption capacity, while N = 0.6793 (less than 1) indicates non-ideal, unfavorable adsorption with a tendency toward cooperative behavior. These results reinforce that the Freundlich model does not adequately capture the adsorption mechanism of amoxicillin onto

IPNs. The Temkin model, which assumes a linear decrease in adsorption energy with increasing surface coverage due to adsorbate–adsorbent interactions, provided a much better fit, with R^2 = 0.9373, closely matching the Langmuir model. This strong correlation implies significant interactions between amoxicillin molecules and the IPNs surface. The Temkin constants, α = 2.8088 L/mg and b_t = 4.3233 J/mol, indicate moderate adsorption energy and further support the notion that chemisorption, rather than physisorption, governs the adsorption process.

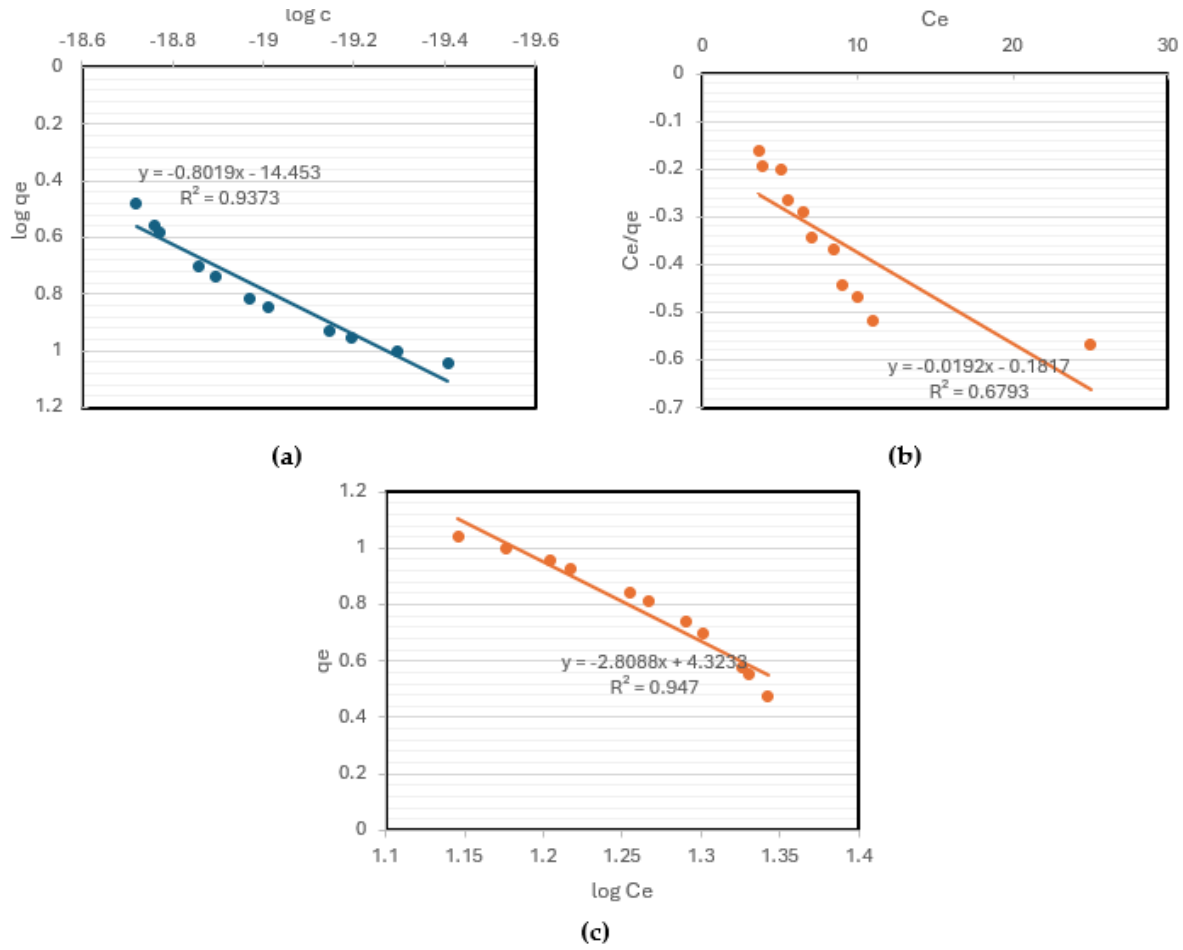

Figure 13. IPNS isotherm model of: (a) Langmuir; (b) Freundlich; (c) Temkin.

Table 1. Isotherm's parameters and correlation coefficients for the adsorption of amoxicillin on IPNS.

Isotherms	Constants	Values
Langmuir	K_L (L/mg)	0.8019
	R_L	14.453
	R^2	0.947
Freundlich	K_f	0.0192
	N	0.6793
	R^2	0.6793
Temkin	α (L/mg)	2.8088
	bt (J/mole)	4.3233
	R^2	0.9373

4. CONCLUSION

This study successfully demonstrated the synthesis and application of IPNs derived from waste disposable polystyrene plates and epoxy resin as a sustainable and cost-effective adsorbent for the removal of amoxicillin from wastewater. The adsorbent was evaluated in a batch reactor under various operational conditions, showing highly favorable adsorption performance. The maximum removal efficiency reached 96% at an optimal dosage of 0.1 g, pH 5, and an initial amoxicillin concentration of 20 mg/L, highlighting the strong potential of IPNs as an effective material for pharmaceutical wastewater treatment.

Kinetic studies indicated that the adsorption of amoxicillin onto IPNs follows a pseudo-second-order model, with a high correlation coefficient (R^2 = 0.9624) and an equilibrium adsorption capacity (q_e) of 8.1342 mg/g, markedly higher than that predicted by the pseudo-first-order model (R^2 = 0.8105, q_e = 1.1951 mg/g). This suggests that the rate-limiting step is governed by chemical adsorption, likely involving covalent bonding or electron exchange between the adsorbent and amoxicillin molecules. Equilibrium isotherm analysis further confirmed that the Langmuir model provided the best fit to the experimental data, implying monolayer adsorption on a relatively homogeneous surface. The Langmuir model exhibited the highest correlation coefficient (R^2 = 0.947) and a K_l value of 0.8019 L/mg, indicating strong affinity between amoxicillin and the IPNs surface. In comparison, the Freundlich model showed poor agreement (R^2 = 0.6793, Kf = 0.0192), suggesting it does not accurately describe the system. The Temkin model, with R^2 = 0.9373 and constants α = 2.8088 L/mg and b_t = 4.3233 J/mol, also indicated that adsorbate–adsorbent interactions contribute to the adsorption process, albeit to a lesser extent than suggested by the Langmuir model.

Overall, the experimental results demonstrate that IPNs are a highly effective, eco-friendly, and cost-efficient adsorbent derived from polymeric waste. This approach provides the dual benefit of removing pharmaceutical contaminants while valorizing plastic waste. The findings establish a strong foundation for future research focused on scaling up IPN production and implementing these materials in continuous wastewater treatment systems.

5. ACKNOWLEDGMENT

We are highly indebted to the Sanitary and Environmental Engineering Department of the Civil Engineering College at the University of Technology- Iraq for providing all the facilities to carry out this work.

6. AUTHORS' NOTE

The author declares that there is no conflict of interest regarding the publication of this article. The author confirmed that the paper was free of plagiarism.

7. REFERENCES

Adeel, M., Grasel Frois, C. F., Berruti, I., Sirtori, C., Malato, S., and Rizzo, L. (2025). Activation of peroxymonosulfate by(sunlight)FeCl3-modified biochar for efficient degradation of contaminants of emerging concern: Comparison with H2O2 and effect of microplastics. *Chemical Engineering Journal*, *507*, 160782.

Al Kindi, G. Y., and Al-Haidri, H. A. (2023). Removal of pharmaceutical residues in 2D and 3D electrochemical processes by using orange peels. *Innovative Infrastructure Solutions*, *8*(6), 171.

Alenzi, A., Hunter, C., Spencer, J., Roberts, J., Craft, J., Pahl, O., and Escudero, A. (2021). Pharmaceuticals' effect and removal, at environmentally relevant concentrations, from sewage sludge during anaerobic digestion. *Bioresource Technology*, *319*, 124102.

Al-Kindi, G. Y., and Al-Haidri, H. A. (2021). The removal of ibuprofen drugs residues from municipal wastewater by Moringa Oleifera Seeds. *Journal of Ecological Engineering*, *22*(1), 83–94.

Al-Kindi, G. Y., and Alnasrawy, S. T. (2022). Tetracycline remove from synthetic wastewater by using several methods. *Journal of Ecological Engineering*, *23*(5), 137-148.

Al-Kindi, G. Y., Ani, F. H. A. L., Al-Bidri, N. K., and Alhaidri, H. A. (2021). Diclofenac removal from wastewater by activated carbon. *IOP Conference Series: Earth and Environmental Science*, *779*(1), 012091.

Chai, W. S., Cheun, J. Y., Kumar, P. S., Mubashir, M., Majeed, Z., Banat, F., Ho, S.-H., and Show, P. L. (2021). A review on conventional and novel materials towards heavy metal adsorption in wastewater treatment application. *Journal of Cleaner Production*, *296*, 126589.

Chen, Z., Zhang, L., Song, Y., He, J., Wu, L., Zhao, C., Xiao, Y., Li, W., Cai, B., Cheng, H., and Li, W. (2015). Hierarchical targeted hepatocyte mitochondrial multifunctional chitosan nanoparticles for anticancer drug delivery. *Biomaterials*, *52*, 240–250.

Codina, A. S., Lumbaque, E. C., and Radjenovic, J. (2025). Electrochemical removal of contaminants of emerging concern with manganese oxide-functionalized graphene sponge electrode. *Chemical Engineering Journal*, *508*, 160940.

Dragan, E. S. (2014). Design and applications of interpenetrating polymer network hydrogels. A review. *Chemical Engineering Journal*, *243*, 572–590.

Fraiha, O., Zaki, N., Hadoudi, N., Salhi, A., ElYoussfi, A., Amhamdi, H., and Ahari, M. (2024). Adsorption-based removal of amoxicillin from aqueous environments: A mini review. *E3S Web of Conferences*, *527*, 03012.

Gao, J., Wu, J., Chen, S. and Chen, Y. (2024). Nitrogen removal from pharmaceutical wastewater using simultaneous nitrification–denitrification coupled with sulfur denitrification in full-scale system. *Bioresource Technology*, *393*, 130066.

Harris, J. D., Wade, E. A., Ellison, E. G., Pena, C. C., Bryant, S. C., McKibben, N. L., and Chase, J. R. (2022). Zinc–Acetate–Amine Complexes as Precursors to ZnO and the Effect of the Amine on Nanoparticle Morphology, Size, and Photocatalytic Activity. *Catalysts*, *12*(10), 1099.

Hayouni, W., Pistre, S., Chkir, N., and Zouari, K. (2025). Contaminants of emerging concern (CECs) as indicators of pollution and hydrological processes in an anthropized

Mediterranean water basin: Case of the Kasserine Basin (Central Tunisia). *Science of The Total Environment*, *984*, 179744.

Hu, J., Liu, Y., Zhang, X., Chen, Z., Tang, M., Lyu, Y., You, X., Helbling, D. E., and Sun, W. (2025). Integrated wide-scope and class-specific nontarget analysis reveals a broad spectrum of organic micropollutants in an urban river. *Water Research*, *285*, 124145.

Ibrahim, T. N. B. T., Feisal, N. A. S., Kamaludin, N. H., Cheah, W. Y., How, V., Bhatnagar, A., Ma, Z., and Show, P. L. (2023). Biological active metabolites from microalgae for healthcare and pharmaceutical industries: A comprehensive review. *Bioresource Technology*, *372*, 128661.

Jin, S.-R., Lee, K.-Y., Park, S.-H., Cheon, J.-M., Kang, S. Bin, and Cho, C.-W. (2025). Amine-functionalized cellulose for the efficient removal of anionic micropollutants from aqueous environments: Development, characterization, and modeling. *Journal of Water Process Engineering*, *75*, 107940.

Kargule, B. B., Al-Asadi, M., Al-Anssari, S., Aljibori, H. S. S., Hamzah, H. T., Tastambek, K. T., Abdullah, T. A., and Abdullah, O. I. (2025). Sustainable removal of dyes from wastewater using eggshell-derived calcium carbonate nanoparticles: Adsorption isotherms, kinetics, and thermodynamic analysis supporting sustainable development goals (SDGs). *ASEAN Journal of Science and Engineering*, *5*(2), 369–394.

Kindi, G. Y. Al, Kadhim, R. J., Azeez, H. S., Abdulrahman, S. M., and Al-Haddad, S. A. (2025). Adsorptive removal of Zinc and Lead Ions from industrial wastewater using Al-Fe Pillared Silty Clay: Kinetic and Isothermal Analysis. *Surfaces and Interfaces, 69*, 106824.

Laksaci, H., Belhamdi, B., Khelifi, O., Khelifi, A., and Trari, M. (2023). Elimination of amoxicillin by adsorption on coffee waste based activated carbon. *Journal of Molecular Structure*, *1274*, 134500.

Lee, K.-Y., Cho, B.-G., Jin, S.-R., Park, S.-H., Cheon, J.-M., and Cho, C.-W. (2025). Experimental characterization and QSAR modeling of maximum uptake and distribution factor for neutral and ionic micropollutants on granular activated carbon in artificial and real wastewaters. *Separation and Purification Technology*, *373*, 133549.

Lin, X., Chan, K., Kingkhambang, K., Hayashi, H., and Zinchenko, A. (2024). Hydrothermal preparation of pharmaceuticals adsorbents from chitin and chitosan: Optimization and mechanism. *Bioresource Technology*, *414*, 131583.

Liu, T., Li, Y., Du, Q., Sun, J., Jiao, Y., Yang, G., Wang, Z., Xia, Y., Zhang, W., Wang, K., Zhu, H., and Wu, D. (2012). Adsorption of methylene blue from aqueous solution by graphene. *Colloids and Surfaces B: Biointerfaces*, *90*, 197–203.

Mohammed, M. N., Abdullah, O. I., Jweeg, M. J., Aljibori, H. S. S., Abdullah, T. A., Alawi, N. M., Rasheed, R. T., Meharban, F., Hamzah, H. T., and Al-Obaidi, Q. (2025). Comprehensive review on wastewater treatment using nanoparticles: Synthesis of iron oxide magnetic nanoparticles, publication trends via bibliometric analysis, applications, enhanced

support strategies, and future perspectives. *ASEAN Journal of Science and Engineering*, *5*(1), 1–30.

Mondal, S., Asif, M. B., Nguyen, T. S., Ismoili, A., and Yavuz, C. T. (2025). Fluorinated porous organic polymers for efficient adsorption of charged organic micropollutants from water. *Polymer*, *333*, 128651.

Munyengabe, A., Banda, M. F., and Augustyn, W. (2025). Predicting plant uptake of potential contaminants of emerging concerns using machine learning models (2018–2025): A global review. *Results in Engineering*, *27*, 106050.

Radu, C.-D., Sandu, I., Diaconescu, R., Bercu, E., and Aldea, H.-A. (2014). Statistic modelling and optimization of the dyeing process of melana fibres with victoria blue b dye in the presence of anionic retarders. *Revista De Chimie*, *65*(7), 797–802.

Sheng, D. P. W., Bilad, M. R., and Shamsuddin, N. (2023). Assessment and optimization of coagulation process in water treatment plant: A review. *ASEAN Journal of Science and Engineering*, *3*(1), 79–100.

Singh, P. K., Bhattacharjya, R., Saxena, A., Thakur, I. S., and Tiwari, A. (2022). Envisaging the role of pharmaceutical contaminant 17-β estradiol on growth and lipid productivity of marine diatom Chaetoceros gracilis. *Bioresource Technology*, *346*, 126642.

Wang, Q., Nie, S., Zietzschmann, F., Rietveld, L. C., Liu, F., Yang, M., and Yu, J. (2025). Mitigating NOM competition against micropollutant adsorption through staged dosing of activated carbon: Loading redistribution of NOM competitors? *Separation and Purification Technology*, *377*, 134270.

Yang, C., Yang, J., Lv, Y., Shi, Y., Cui, D., Yin, M., Li, L., Zhang, J., and Xu, C. (2025). Suspect and non-target screening for emerging contaminants of potential concern and risk assessment in wastewater treatment plants: A case study of a typical industrial city in China. *Science of The Total Environment*, *989*, 179857.